

We are IntechOpen, the world's leading publisher of Open Access books Built by scientists, for scientists

6,900

Open access books available

186,000

International authors and editors

200M

Downloads

Our authors are among the

154

Countries delivered to

TOP 1%

most cited scientists

12.2%

Contributors from top 500 universities



WEB OF SCIENCE™

Selection of our books indexed in the Book Citation Index
in Web of Science™ Core Collection (BKCI)

Interested in publishing with us?
Contact book.department@intechopen.com

Numbers displayed above are based on latest data collected.
For more information visit www.intechopen.com



Activity-Artifact Flow of GPS/INS Integration for Positioning Error De-Correlation

Xiaoying Kong, Li Liu and Heung-Gyoon Ryu

Additional information is available at the end of the chapter

<http://dx.doi.org/10.5772/50516>

1. Introduction

Vehicle positioning systems are composed of positioning sensors and positioning algorithms. Positioning sensors provide direct or indirect position, velocity, attitude and timing information. Positioning algorithms transfer sensor direct readings to desired positioning information. Positioning sensors are classified into absolute sensors and dead reckoning sensors (Sukkarieh, 2000). Absolute sensors directly provide the relationships between vehicle position and external positioning references. Dead reckoning sensors measure the vehicle's position and orientation increment to its last moment without external references. Global Navigation Satellite System (GNSS) is a widely used absolute positioning system using external satellite references. Inertial Navigation System (INS) is an example of dead reckoning positioning system. INS uses inertial measurement unit (IMU) to measure the self-contained position changing rate, then computes the desired positioning information. INS has been employed in navigation for rockets, missiles, aircrafts, land vehicles, ocean vessels and robots.

These two types of positioning sensors have their own characteristics. For example, Global Positioning System (GPS), one of the GNSSs, provides positioning and timing information to world-wide users. GPS has played an important role in national security, economic growth, transportation safety, and critical national infrastructure (GAO, 2009). However GPS sometimes suffers accuracy and availability problems. INS provides self-contained high frequency positioning information by integration of accelerations and rotation rates. During the integration process, any bias and errors in IMU sensors will be amplified over time. This results in the unbounded growth of positioning errors in the entire real time computing process.

Considering these sensor characteristics, many efforts have been made to aim for higher quality positioning achievement. There are two levels of research efforts. At low level or

component level, hardware and infrastructure improvement, sensor error modelling techniques have been studied (Nebot et al., 1996; Nebot et al., 1999; Kong et al., 1999). At high level or system level, integrations of two types of sensors are developed as positioning system architectures (Nebot et al., 1996; Scheduling, 1997, Scheduling et al., 1997, Sukkarieh, 2000).

Research and development efforts on GPS quality improvement include: launching new satellites (GAO, 2009; Committee on Oversight and Government Reform, 2009); deploying Differential GPS (GPS) and Wide Area Augmentation System (WAAS) infrastructures to improve GPS accuracy and availability (Wikipedia Differential GPS, 2012; Federal Aviation Administration, 2012); modelling GPS multi path effects (Gaylor et al., 2005; Wu & Hsieh, 2010); mitigating GPS errors in high-interference environment (Groves, 2005); modelling ionospheric effects (Rose et al., 2009); analyzing unintentional interference (Owen & Wells, 2001); modelling GPS signal blockage (Gaylor et al., 2005); and modelling GPS external behaviours (Nebot et al., 1996; Kong et al., 2010).

Efforts on INS improvements include: developing new types of INS using new mechanisms such as developing new optical IMU; developing low cost IMU such as MEMS (Microelectromechanical systems) IMU and associated algorithms to extend user services (Geiger et al., 2008; Sahawneh & Jarrah 2008); developing high quality IMU testing facilities; modelling IMU biases; modelling INS errors in initial alignment stages (Nebot et al., 1996; Kong et al., 1999); improving INS error propagation models during positioning missions (Kong et al., 1999).

Besides the positioning sensor research, on system level, integrating two types of sensors to form an improved positioning system has been a major effort in positioning research. In literature, GPS/INS integration approaches have been widely adopted and can be classified to uncoupled, loosely coupled, and tightly coupled integrations (Sukkarieh, 2000). In uncoupled systems, GPS and INS work independently. Loosely coupled systems integrate GPS and INS provided positioning information without feedback to GPS or INS. In tightly coupled system, direct measurements from GPS or INS, and computed information are integrated. Real time feedbacks are provided to GPS or INS. Recently, ultra-tight integration has emerged. On ultra-tight integration architecture, INS, GPS phase, frequency and code tracking loops are integrated deeply to improve GPS performance (Alban et al., 2003; Lashley et al., 2010).

The GPS/INS integration is usually implemented using a filter such as Kalman filter. From the view point of filter mechanism, the above GPS/INS integration approaches could also be classified to feedforward filter and feedback filter (Maybeck, 1979; Sukkarieh, 2000). In a feedforward filter approach, the filter estimates the desired positioning or error states. These filter outputs are not fed back to GPS or INS measurements for real time correction. The positive aspect of feedforward filter is that if the filter fails, the sensor measurement information is still available. But the INS errors will grow over time due to the integration of INS bias drift (Maybeck, 1979). A feedback filter allows filter estimations to feedback to sensors for measurement correction. The INS information is bounded over time by real time

error feedback and correction. Under the feedback and feedforward filter types, there are direct filter and indirect filter depending on the filter outputs. Direct filters output positioning readings directly. Indirect filters output positioning error estimates.

We use an entity-relationship model to analyze and classify the GPS/INS integration concepts as in Fig. 1.

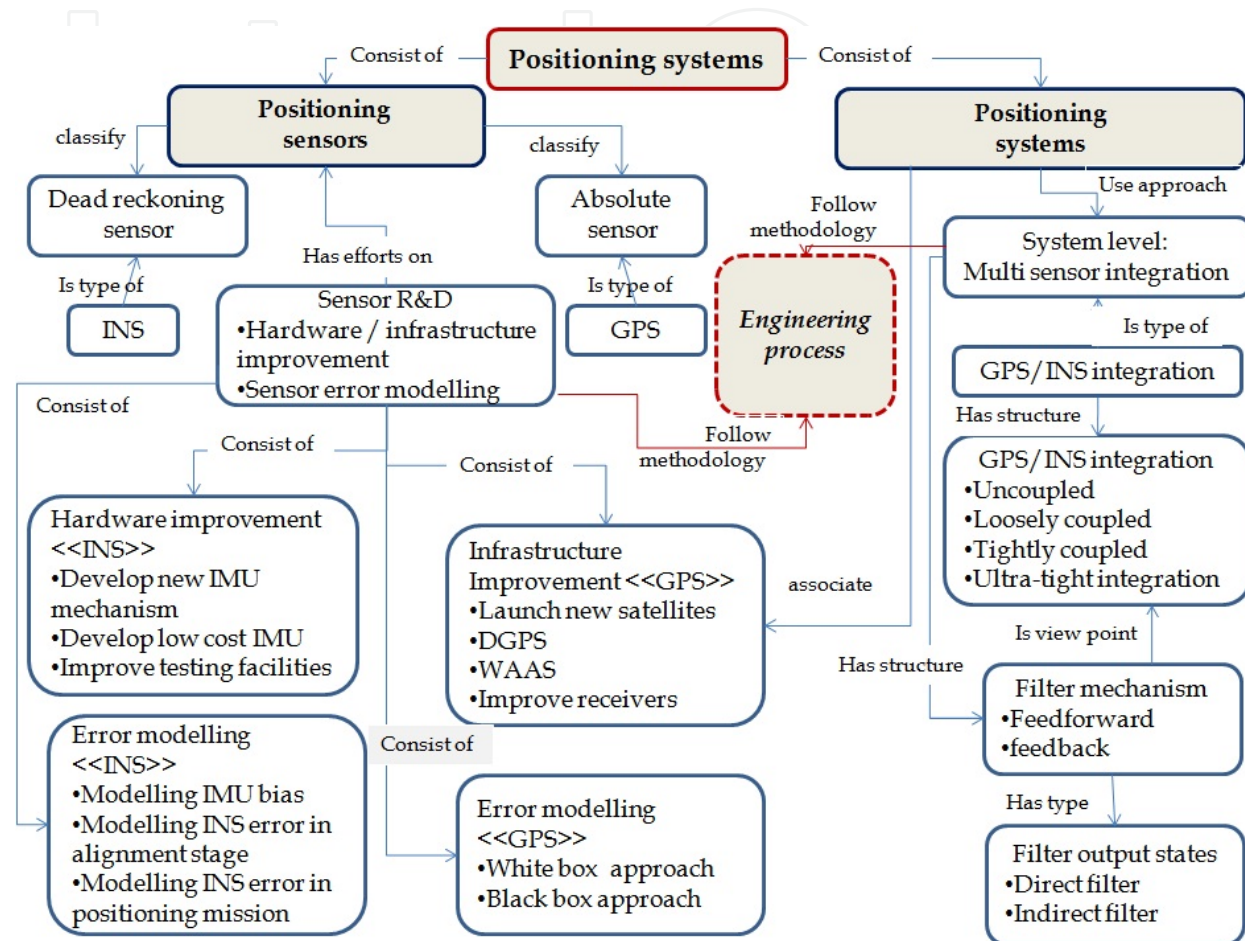


Figure 1. Classifications of positioning system research using GPS/INS integration

This chapter presents a GPS/INS integration approach for positioning error de-correlation by analyzing system filter structure and performance. It is from the view point of implementing feedforward and feedback structures. The aim of this approach is to improve the positioning quality of the GPS/INS integration system in accuracy and availability aspects. The contributions of this research fill in the gap in the above classification map in both positioning sensor level and system level. A new engineering process based on the practice in this research is proposed in this chapter. The new engineering process is added into the map as a new classification entity.

To present this research in this chapter, a bottom-top approach is used to describe this GPS/INS positioning system integration process. In the following sections, we start from component level presentation by analysing sensor models in Section 2. System level design and system performance verification are presented in Sections 3 and 4. Section 3 presents the

feedforward filter approach in frequency domain and time domain. Feedback filter approach is discussed in Section 4. Based on the engineering practices in Sections 2, 3 and 4, an engineering process with research activities and associated artifacts is formed and summarized. Section 6 draws the conclusion.

2. Modelling GPS error using shaping filter

In the GPS/INS integration approach presented in this chapter, GPS is chosen to be the main positioning sensor. INS aids GPS. Nowadays GPS receivers are available in market with relatively low cost. INS accuracy level and cost level vary in relatively wide range. GPS receivers could be purchased first. INS accuracy level could be decided by analyzing GPS/INS filter performance before purchasing decision making. Once a GPS receiver is ready for system implementation, GPS positioning performance could be analyzed by modelling GPS errors. GPS positioning quality could be improved then by using INS aiding.

In literature, GPS error modelling has been focusing on understanding GPS signal error sources. Major efforts are on modelling the characteristics of GPS multi path effects (Gaylor et al., 2005; Wu & Hsieh, 2010), ionospheric effects (Rose et al., 2009), unintentional interference (Owen & Wells, 2001), high-interference environment (Groves, 2005), and GPS signal blockage (Gaylor et al., 2005). These approaches look at the internal aspects of GPS errors. We refer to these as “white box” modelling approach. Another type of research looks at the external behaviours of GPS errors. GPS errors are modelled using shaping filter in frequency domain (Maybeck, 1979; Nebot et al., 1996; Kong et al., 2010). This approach could be referred as “black box” approach. In this chapter, we use black-box approach to understand GPS errors.

GPS measured information includes time and pseudo range to satellite. Latitude and longitude of GPS receiver’s position are calculated using pseudoranges to a number of satellites. It was found that the errors of GPS calculated positions show the characteristics of colour noise (Nebot et al., 1996). In the approach of this chapter, we wrap the entire calculated position errors as a black-box from external user’s view point. The entire GPS calculated position errors are modelled as colour noise using shaping filter.

Shaping filter models colour noise as a linear system driven by white noise (Maybeck, 1979). Measurement errors are the output of the shaping filter. The form of a shaping filter could be examined using Power Spectral Density (PSD) in frequency domain. GPS error modelling using shaping filter with PSD is explained as follows.

From external user’s view point, GPS measurement errors include satellite signal biases and receiver noises. On satellite bias side, satellite constellation could be changed if some satellites are de-orbited or new satellites are launched (GAO, 2009). Selective Availability (SA) was intentionally introduced to degrade positioning accuracy (Wikipedia, Differential GPS, 2012). From GPS receiver’s side, user receivers could be purchased from different vendors with different quality. The factors from the two sides will affect the GPS measurement errors’ frequency characteristics. Therefore GPS errors using shaping filter

should be modelled with a particular receiver under the current satellite constellation. We take two cases as examples for shaping filter analysis. Stand-alone GPS is considered for vehicles in areas without the coverage of DGPS and WAAS.

Case 1: Stand-alone GPS signal with Selective Availability error; receiver type 1.

Case 2: Stand-alone GPS signal without Selective Availability; receiver type 2.

By examine the PSD curves of GPS position errors in Case 1, we found the GPS error shows the characteristics of a second order system. Transfer positioning errors to east-north-down frame. For axis x (east) as an example, the shaping filter of GPS error can be presented as in Fig. 2 (a).

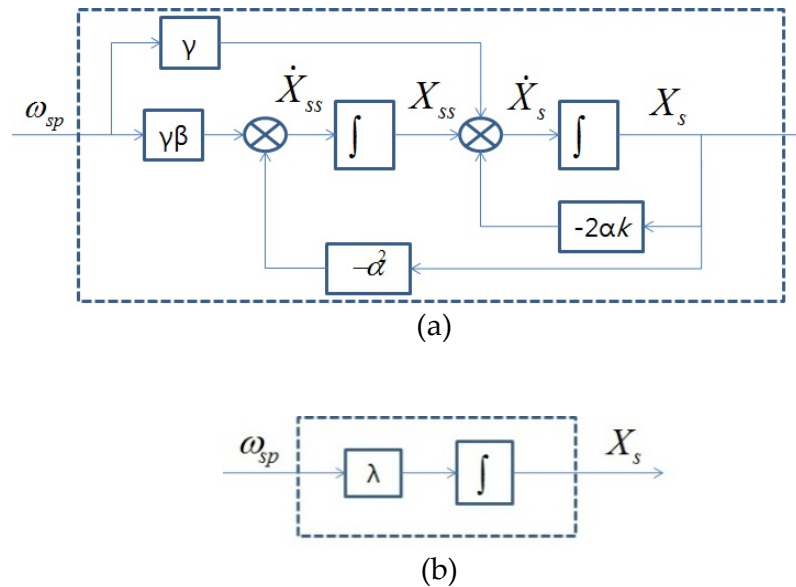


Figure 2. (a) Shaping filter with a second order system (b) Shaping filter with a first order system

In this shaping filter structure, ω_{sp} is the input of the shaping filter. ω_{sp} is a unity white noise. X_s is the output of the shaping filter. X_s represents the GPS colour noise. α , β , γ and k are filter parameters obtained by experimental data sets during PSD curve fitting (Kong et al., 2010). This shaping filter could be presented in state space as the following second order system:

$$\begin{aligned} \dot{X}_s(t) &= -2\alpha k X_s(t) + X_{ss}(t) + r\omega_{sp}(t) \\ \dot{X}_{ss}(t) &= -\alpha^2 X_{ss}(t) + r\beta\omega_{sp}(t) \end{aligned} \quad (1)$$

For Case 2, the shaping filter is experimentally obtained as a first order system as in Fig. 2 (b). The state space form of Case 2 is presented as in Equation (2).

$$\dot{X}_s(t) = \lambda\omega_{sp}(t) \quad (2)$$

The aim of the shaping filter is to duplicate the GPS measurement errors. The GPS positioning could be constructed using an augmented system with the shaping filter. The

augmented system is constructed with a $m \times 1$ state vector $x(t)$, a $p \times 1$ measurement vector $z(t)$, a $q \times 1$ white noise vector $w(t)$ on process model. Using the second order shaping filter as an example, the augmented system is as Fig. 3. The augmented system is presented using the following equation:

$$\begin{aligned} \dot{x}(t) &= F(t)x(t) + G(t)w(t) \\ z(t) &= H(t)x(t) + n_s(t) + \tau_{gps}(t) \end{aligned} \tag{3}$$

where x is the system state. w is white noise. z is the system measurement. z is corrupted by colour noise n_s and white noise τ_{gps} . n_s is presented as:

$$n_s(t) = X_s(t) \tag{4}$$

where X_s is the output of the shaping filter described in Fig. 2 (a).

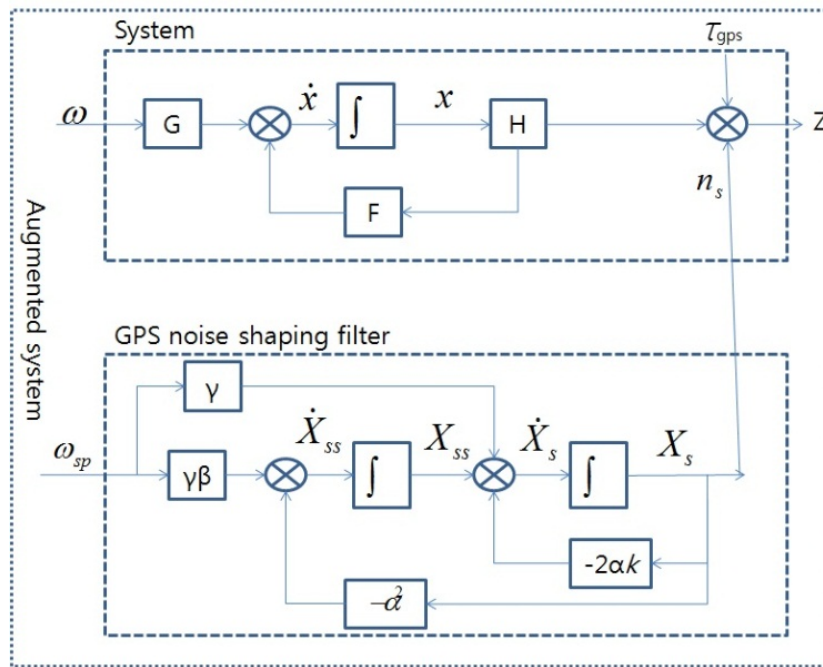


Figure 3. Augmented system with shaping filter duplicating GPS measurement noises

As in Fig. 3, the augmented state x_s can be defined as follows:

$$x_s(t) = \begin{bmatrix} x(t) \\ X_s(t) \\ X_{ss}(t) \end{bmatrix} \tag{5}$$

The process model of the augmented system can be described as:

$$\dot{x}_s(t) = \begin{bmatrix} F(t) & 0_{m \times 2} & 0_{m \times 2} \\ 0_{1 \times m} & -2\alpha k & 1 \\ 0_{1 \times m} & -\alpha^2 & 0 \end{bmatrix} \begin{bmatrix} x(t) \\ X_s(t) \\ X_{ss}(t) \end{bmatrix} + \begin{bmatrix} G & 0_{q \times 1} \\ 0_{1 \times q} & r \\ 0_{1 \times q} & r\beta \end{bmatrix} \begin{bmatrix} w(t) \\ w_{sp}(t) \end{bmatrix} \tag{6}$$

The observation model of the augmented system is:

$$z(t) = \begin{bmatrix} H(t) & I_p 0_p \end{bmatrix} \begin{bmatrix} x(t) \\ X_s(t) \\ X_{ss}(t) \end{bmatrix} + \tau_{gps}(t) \quad (7)$$

Once the augmented system is constructed, INS could be used to aid de-correlating the GPS errors. In the following sections, de-correlating approach is described using two types of filters: feedforward filter and feedback filter.

3. GPS error de-correlation process using feedforward filter

INS is chosen to aid GPS to estimate and remove colour noises. We call this process as GPS error de-correlation process. INS measurements also contain noises. Feedback filter approach uses filter estimation to correct INS noises in real time. Feedforward filter approach leaves the INS noises without feedback correction. If the filter fails, INS is able to provide positioning independently in feedforward structure. In this section, we consider feedforward filter approach first. Feedback approach will be described in the next section.

3.1. Feedforward filter structure

Fig. 4 is a GPS/INS integration feedforward filter structure. INS indicated positioning information and GPS measurements are integrated into the system integration filter. The system filter estimates the velocity errors, position errors, shaping filter states, and outputs the position information. There is no feedback of position error estimation to sensors for real time correction.

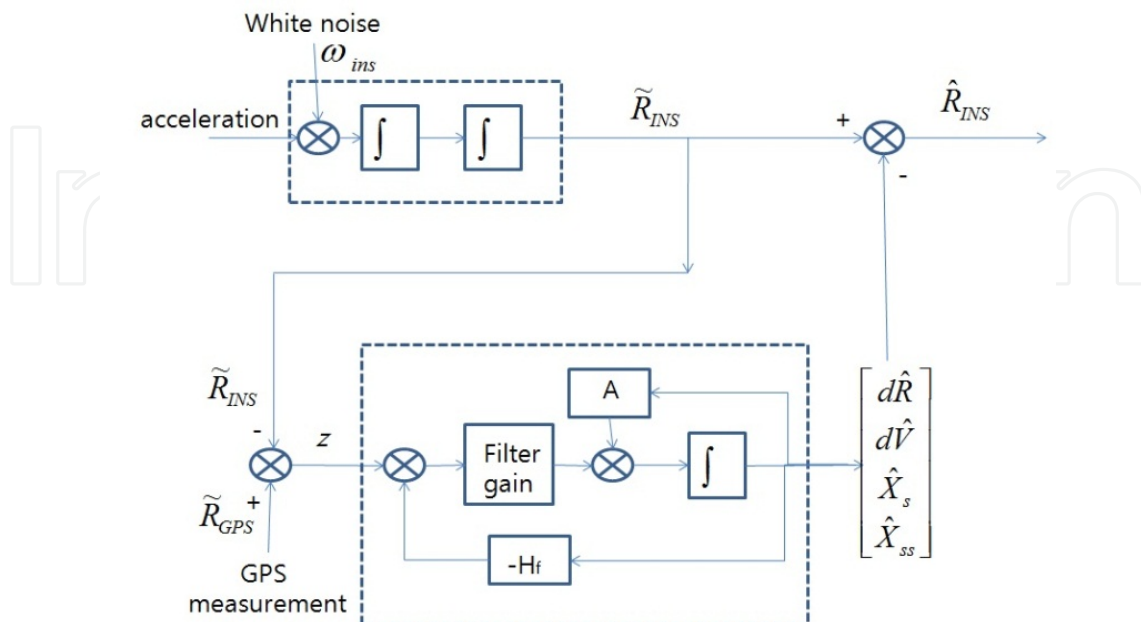


Figure 4. Feedforward filter structure

To focus on GPS error de-correlation process using this feedforward filter, we assume that the INS coordinate system is already transformed into the GPS coordinate system using gyros' information. The INS positioning reading is computed by integrating acceleration twice. The acceleration noise is assumed driven by white noise. Using the case of the second order shaping filter as example, Fig. 4 illustrates the filter inputs, outputs and state estimates.

The state of this feedforward filter is:

$$x(t) = [dR(t), dV(t), X_s(t), X_{ss}(t)]^T \quad (8)$$

The velocity error and position error in the filter state are defined as:

$$\begin{aligned} dR(t) &= \tilde{R}_{INS}(t) - R_{true}(t) \\ dV(t) &= \tilde{V}_{INS}(t) - V_{true}(t) \end{aligned} \quad (9)$$

where $R_{true}(t), V_{true}(t)$ are vehicle true position and velocity. $\tilde{R}_{INS}(t), \tilde{V}_{INS}(t)$ are INS computed position and velocity.

The filter observation $z(t)$ is the difference between the GPS output and INS output.

$$z(t) = \tilde{R}_{GPS}(t) - \tilde{R}_{INS}(t) \quad (10)$$

As described in the previous section, GPS outputs are modelled as the true position corrupted by colour noise X_s driven by white noise.

From Fig. 4, the following relationships can be derived:

$$\begin{aligned} d\dot{R}(t) &= dV(t) \\ d\dot{V}(t) &= \omega_{ins}(t) \end{aligned} \quad (11)$$

And

$$\begin{aligned} z(t) &= [R_{true}(t) + X_s(t) + \tau_{gps}(t)] - [R_{true}(t) + dR(t)] \\ &= -dR(t) + X_s(t) + \tau_{gps}(t) \end{aligned} \quad (12)$$

The de-correlation filter process model is therefore given by:

$$\dot{x}(t) = \begin{bmatrix} d\dot{R}(t) \\ d\dot{V}(t) \\ \dot{X}_s(t) \\ \dot{X}_{ss}(t) \end{bmatrix} = \begin{bmatrix} 0 & 1 & 0 & 0 \\ 0 & 0 & 0 & 0 \\ 0 & 0 & -2\alpha k & 1 \\ 0 & 0 & -\alpha^2 & 0 \end{bmatrix} \begin{bmatrix} dR(t) \\ dV(t) \\ X_s(t) \\ X_{ss}(t) \end{bmatrix} + \begin{bmatrix} 0 & 0 \\ 1 & 0 \\ 0 & \gamma \\ 0 & \gamma\beta \end{bmatrix} \begin{bmatrix} \omega_{ins}(t) \\ \omega_{sp}(t) \end{bmatrix} \quad (13)$$

The observation model of the filter is given by:

$$z(t) = H_f x(t) + \tau_{gps}(t) \quad (14)$$

where

$$H_f = [-1 \ 0 \ 1 \ 0] \quad (15)$$

The covariance matrices of the process and observation noises are

$$\begin{aligned} Q &= E[w(t)w^T(t+\tau)] = \begin{bmatrix} q_{ins}^2 & 0 \\ 0 & 1 \end{bmatrix} \delta(\tau) \\ R &= E[\tau_{gps}(t)\tau_{gps}^T(t+\tau)] = \sigma_{GPS}^2 \delta(\tau) \end{aligned} \quad (16)$$

with the white noise variance q_{ins}^2 on the acceleration output and the variance σ_{GPS}^2 on the GPS position observation.

Equations (13) ~ (16) compose the feedforward de-correlation filter. In the next section, this feedforward filter will be analyzed in frequency domain and time domain respectively.

3.2. Analysis of de-correlation process using feedforward filter

The GPS/INS integration feedforward filter structure is described in the previous section. In this section, the positioning error de-correlation process is demonstrated in frequency domain and time domain. The de-correlation process is designed as the following procedure in Table 1.

Step	Domain	Research Details
Step 1	frequency domain	The filter transfer function from the observation $z(s)$ to the filter state estimates $x(s)$ is calculated.
Step 2	frequency domain	Tuning the filter noises levels, the gain of the filter transfer function is analysed using bode plots. INS noise levels are tuned during this step.
Step 3	time domain	The performance of the filter is analyzed at positioning system level. The shaping state time series and GPS error time series are compared. The system error level is examined.
Step 4	Iterative in both frequency and time domains	Continue tuning of the noise levels at Step 2 and analyzing time domain performance at Step 4. The de-correlation process is successful until the system error is tuned to the required level.

Table 1. Procedure of the positioning error de-correlation process in frequency domain and time domain

Using the feedforward filter structure in Fig. 4 and following the procedure in Table 1, the de-correlation process is demonstrated as below.

Step 1:

As illustrated in Fig. 4, in frequency domain, the transfer function from the observation $z(s)$ to the filter state estimate is calculated by:

$$\frac{\hat{x}(s)}{z(s)} = (sI_{4 \times 4} - A + KH_f)^{-1}K \tag{17}$$

where the filter-gain K is determined by the filter parameters and the noises of the filter process and observation.

and

$$A = \begin{bmatrix} 0 & 1 & 0 & 0 \\ 0 & 0 & 0 & 0 \\ 0 & 0 & -2\alpha k & 1 \\ 0 & 0 & -\alpha^2 & 0 \end{bmatrix} \tag{18}$$

Step 2:

The sensor noise levels are tuned in the filter. In the Case 1 for the filter in Fig. 4, a stand-alone GPS without differential correction is chosen. The variance of the position error is about $20 \times 20 m^2$. The noise level of INS is tuned during this de-correlation analysis process before INS purchasing decision. For the example of Case 1, the range of accelerometer's noise variance is tuned from $1 \times 10^{-2} (m/s^2)^2$ to $1 \times 10^{-6} (m/s^2)^2$.

Fig. 5 is the bode plot by tuning an accelerometer with a variance of $1 \times 10^{-2} (m/s^2)^2$. The gain of the shaping state estimate \hat{X}_s is very small.

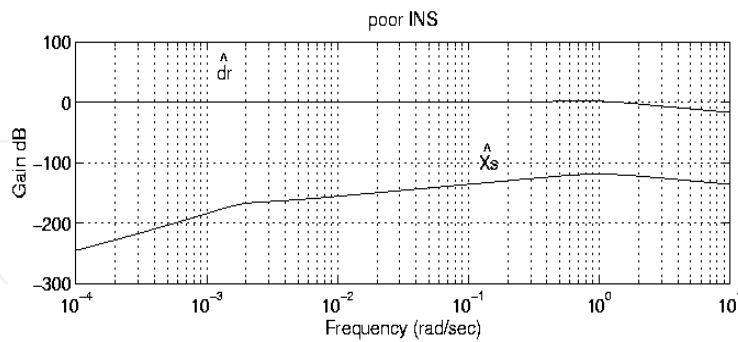


Figure 5. Bode plot of the feedforward filter using a low quality accelerometer

Step 3:

Switching to time domain, using the parameters in Step 2, the time series of GPS position estimates, error estimates, and shaping state estimates are illustrated in Fig. 6.

In the example of Case 1, the vehicle is in stationary state. The GPS measurement output consists of the entire colour noise. As in Fig. 6(a), the shaping state estimates do not follow

the shape of the GPS measurements. Fig. 6(b) illustrates the system position estimates follow the INS position outputs. The position error estimates grow over time without bound in feedforward filter. De-correlation fails using this accelerometer quality level.

Step 4:

We iteratively tune the feedforward filter by adjusting sensor noise level using Step 2 and Step 3. Until in frequency domain, the gain of the shaping state in bode plot approaches 0dB, the de-correlation process is successful.

Fig. 7 is a successful de-correlation example of bode plot using an accelerometer with a variance of $1 \times 10^{-6} (m/s^2)^2$. The gain for the shaping state estimate \hat{X}_s within $10^{-4} rad/sec$ to $10^{-2} rad/sec$ is approaching 0dB. Examine the time domain performance for this case, Fig. 8 shows that the time series of the shaping state estimate \hat{X}_s follows the shape of the GPS output. The system position estimate errors are reduced to 4m.

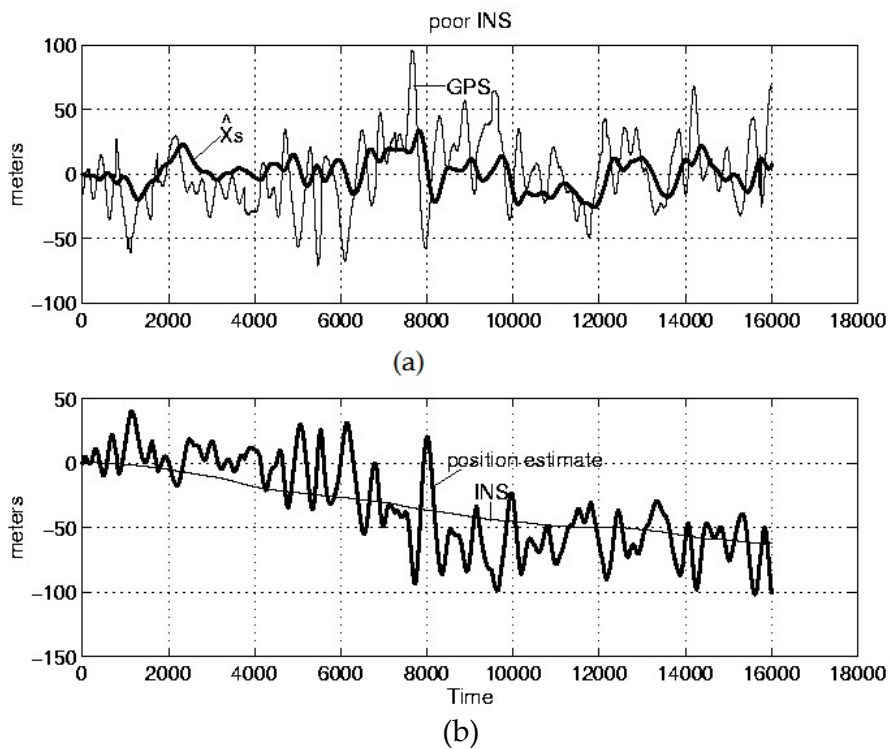


Figure 6. Time domain results using a low quality accelerometer (Unit: data iteration – meter) (a)Time domain performance of shaping filter estimate and GPS error measurement (b)Time domain performance of INS position estimate and system position estimate

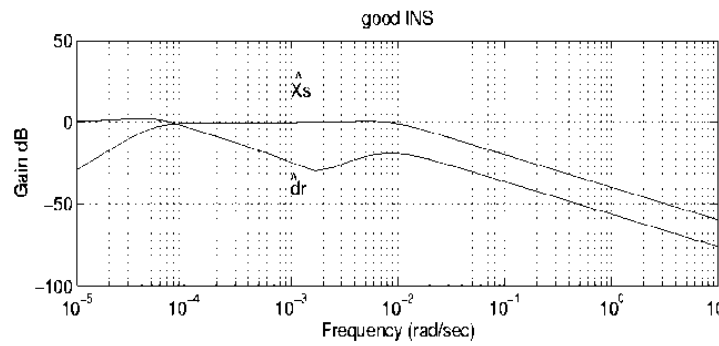


Figure 7. Bode plot of the feedforward filter using a high quality accelerometer

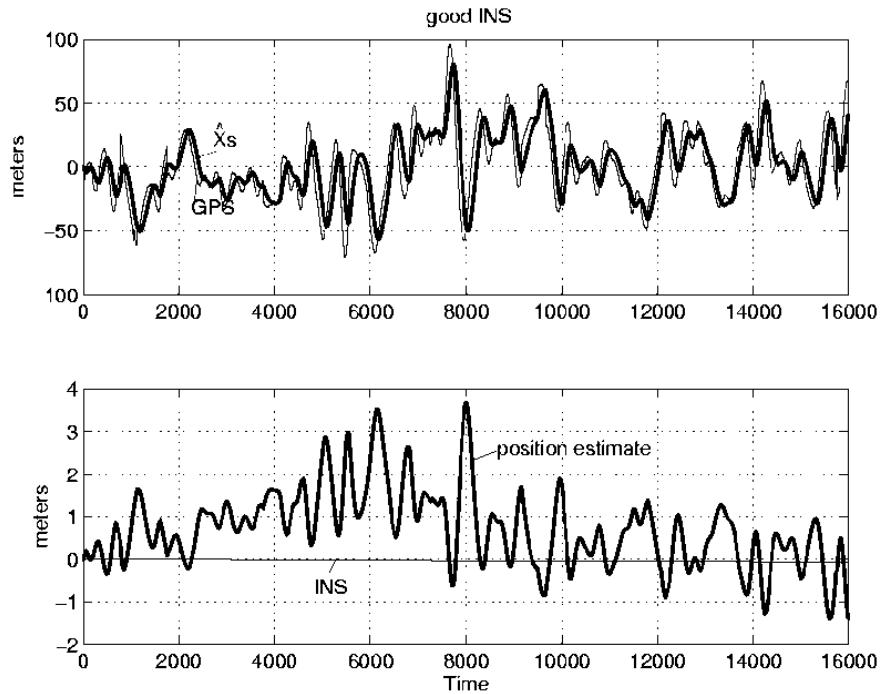


Figure 8. Time domain results using a high quality accelerometer (Unit: data iteration – meter)

During the filter tuning process using Step 2 to Step 4, the INS quality requirement for the successful de-correlation can be found from the bode plot of the filter transfer function. From the experiments we found that in order to use a feedforward filter to de-correlate GPS colour noises using an INS, the accuracy level of the INS should be above $3.16 \times 10^{-6} (m/s^2)^2$ on variance of the accelerometers.

The feedforward filter is able to output position estimates directly. The GPS and INS are integrated loosely. If the system integration filter fails, the INS is still able to provide positioning information without the filter. But there is no feedback to correct errors in INS in real time. The position outputs will grow over time due to the step by step integration of the inertial sensor's drift errors. Once a feedback scheme is introduced to the filter, the INS error could be reduced and the system position outputs could be bound. This feedback scheme is implemented in feedback filter.

4. GPS error de-correlation process using feedback filter

4.1. Feedback filter structure

A feedback scheme for inertial sensor correction is able to overcome the position error growth. Fig. 9 is a feedback filter structure. The GPS and INS are integrated tightly.

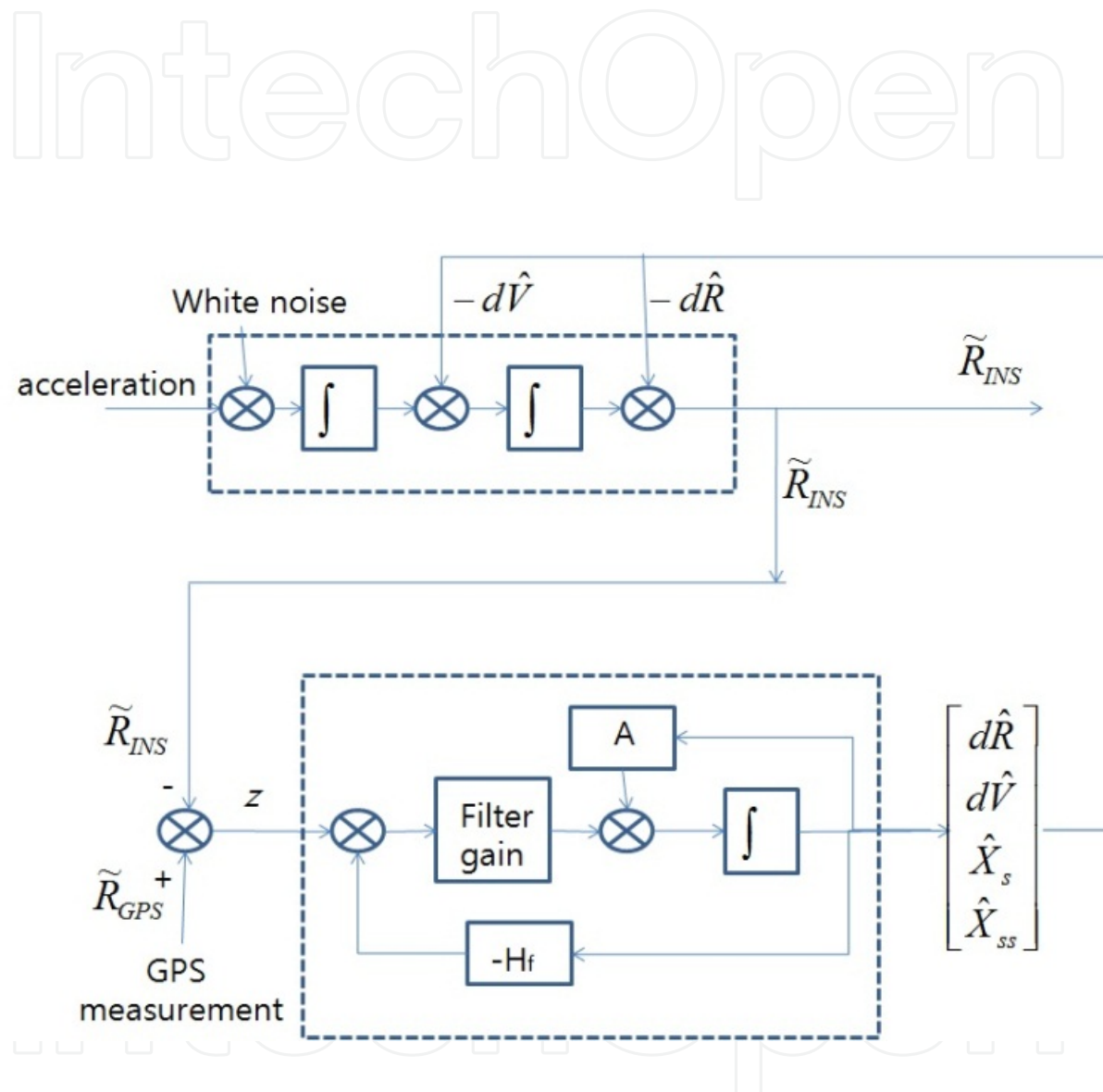


Figure 9. Feedback filter structure

In this feedback filter structure, the filter outputs the estimates of position error $d\hat{R}$, velocity error $d\hat{V}$, and shaping state estimation. Using the second order shaping filter as an example, the shaping states estimation include two states \hat{X}_s and \hat{X}_{ss} . If using the first order shaping filter, the feedback filter will output one shaping state estimate \hat{X}_s .

INS computes the velocity by integration acceleration. INS position is computed by integration the computed velocity. The filter then takes the input from the measurement difference between GPS and INS. The filter estimates the errors of velocity, position and GPS errors. The estimated velocity error and position error are feedback to INS computing process for correction as illustrated in Fig. 9. The filter states are still $[dR(t), dV(t), X_s(t), X_{ss}(t)]$ if using the second order shaping filter. The process model remains the same as the feedforward filter in Equation (13), and the observation model is the same as shown in Equations (14) and (15).

4.2. Feedback filter analysis in frequency domain and time domain

Following the same procedures in Table 1, the positioning system error de-correlation process using feedback filter is analyzed and implemented as follows.

In frequency domain, the filter transfer function from the observation to filter states is calculated. The filter is tuned using a range of accelerometers' error levels. Bode plots at each level are plotted. The gains of shaping states are analyzed. Fig. 10 shows the bode plot using a low quality accelerometer with a noise variance of $1 \times 10^{-2} (m/s^2)^2$.

Fig. 10 shows the gain of the shaping state estimate on the bode plot is very low. The ratio of the shaping estimate to the GPS error measurement is lower than 1. Using the parameters of this level to calculate the time series of shaping state, position estimates, error estimates, the time domain performance are illustrated in Fig. 11. Fig. 11(a) shows the shaping state estimates do not follow the shape of GPS errors. Fig. 11(b) shows the INS position estimate errors are bound over time due to the error feedback and INS correction. The system error de-correlation is unsuccessful using this quality level of accelerometer.

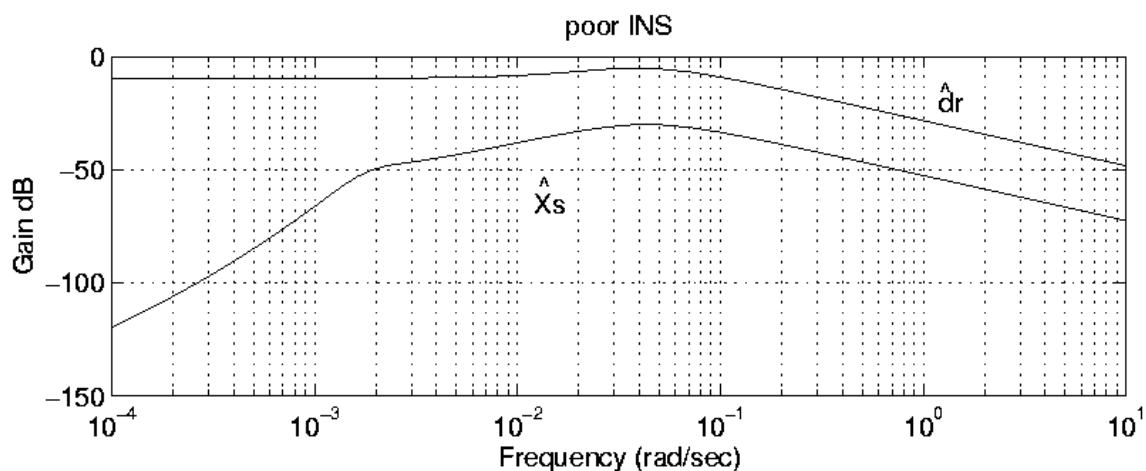


Figure 10. Bode plot of the feedback filter using a low quality accelerometer

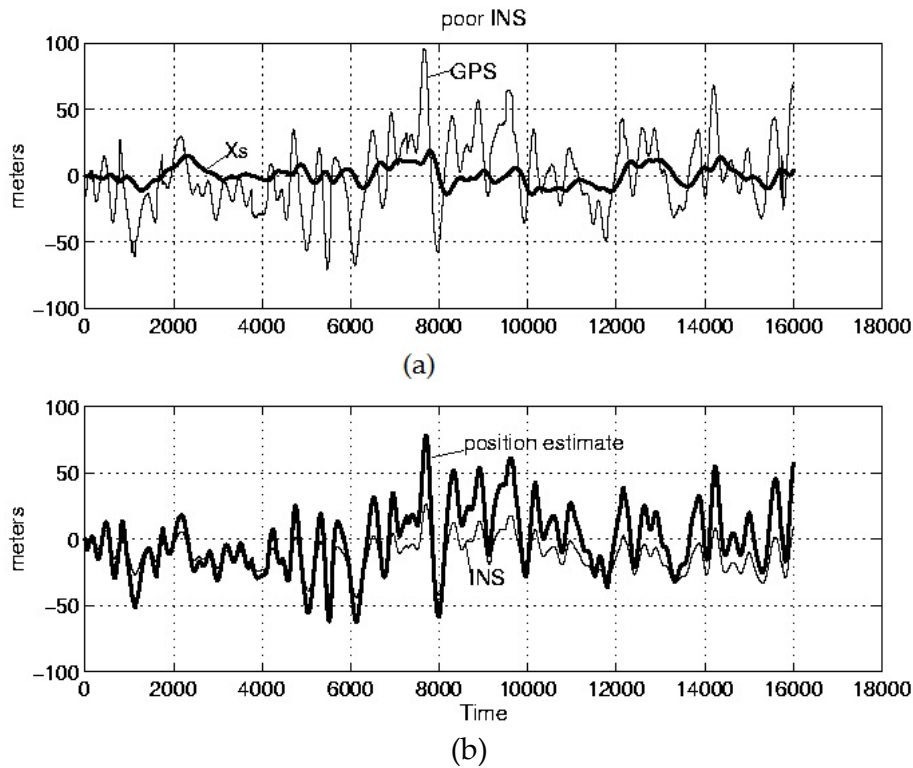


Figure 11. Feedback filter performance in time domain using a low quality accelerometer (Unit: data iteration -meter) (a)Time domain performance of shaping filter estimate and GPS error measurement (b)Time domain performance of INS position estimate and system position estimate

Continually tuning the feedback filter by trying different levels of accelerometer variance levels following Step 2 and Step 3 in Table 1, the best gain could be found in bode plot of the transfer function. Fig. 12 is a bode plot using an accelerometer variance of $1 \times 10^{-6} (m/s^2)^2$. The gain of the shaping state estimate to observation is approaching 0dB within $3 \times 10^{-4} rad/sec$ to $10^{-2} rad/sec$. As shown in Fig. 13 in time domain, the shaping state estimates track the GPS error shapes and match their magnitudes in time series.

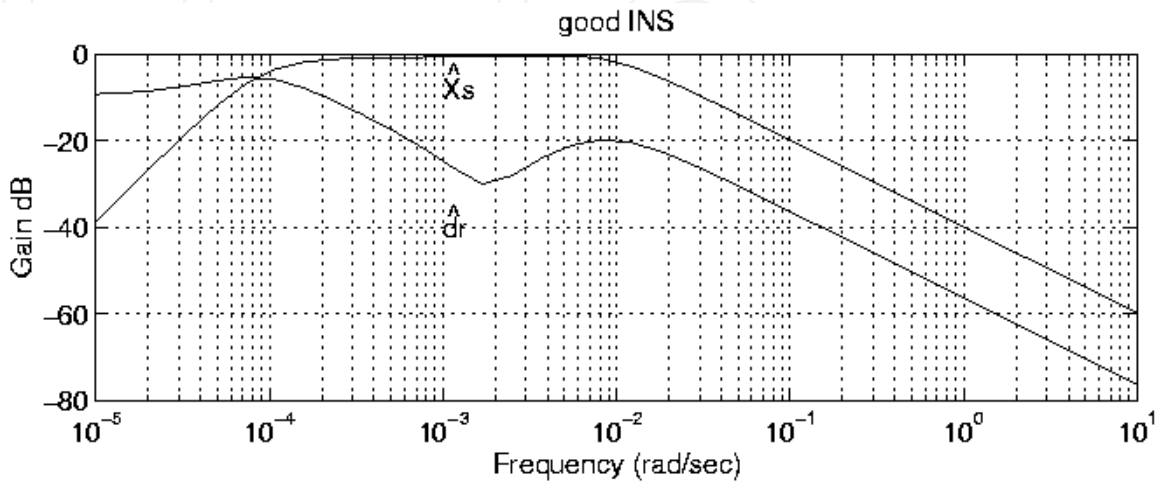


Figure 12. Bode plot of the feedback filter using a high quality accelerometer

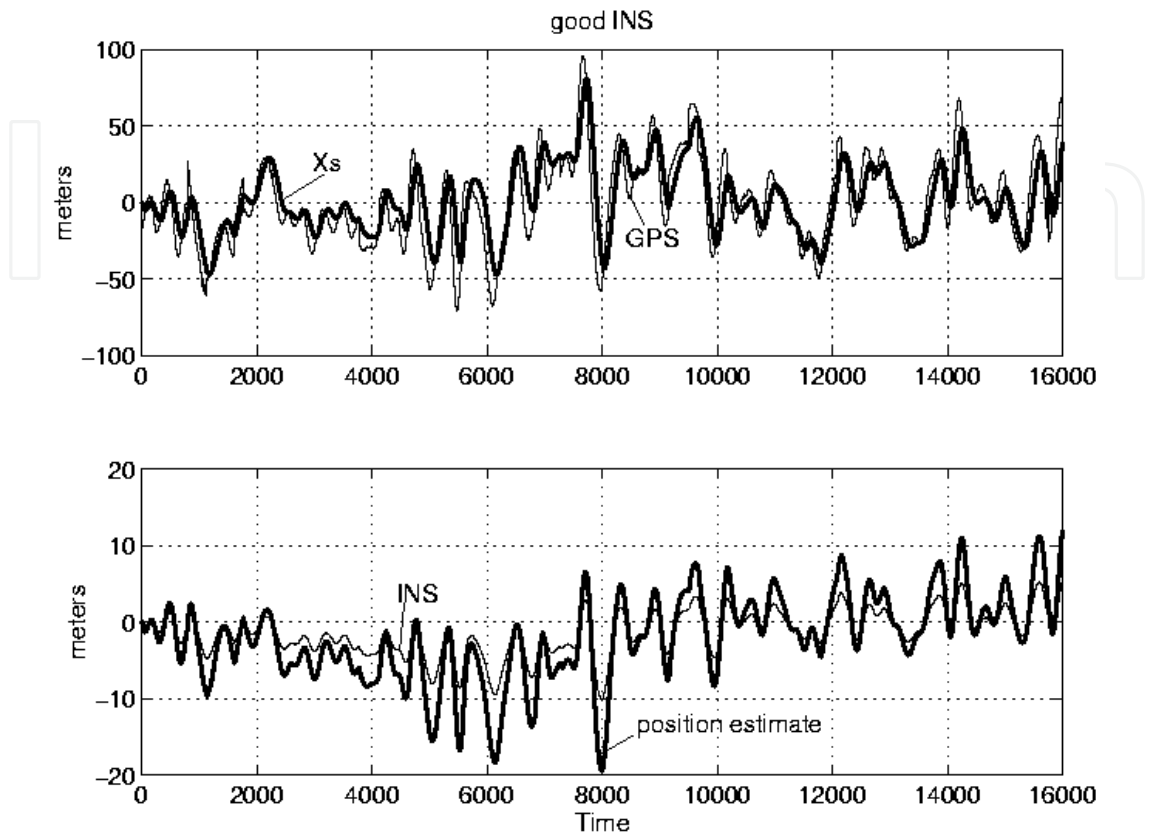


Figure 13. Feedback filter time domain performance using a high quality accelerometer (Unit: data iteration – meter)

In this feedback filter tuning process, we found that the accelerometer variance threshold for GPS error de-correlation using a stand-alone GPS with error variance of $20 \times 20 m^2$ is $3.16 \times 10^{-6} (m/s^2)^2$.

Compare with the de-correlation threshold finding in the feedforward filter, the quality requirements based on accelerometer variance level are the same for both feedforward filter and feedback filter. The benefit of the feedback approach is that the position estimates are bound over time using the feedback filter structure.

5. Engineering process of the positioning error de-correlation approach

To effectively reuse the artifacts and minimize the designing efforts in both feedforward and feedback approaches, this GPS error de-correlation approach could be standardized using an activity-artifact flow to form a repeatable engineering process. Fig. 14 shows the activities and associated artifacts of this engineering process.

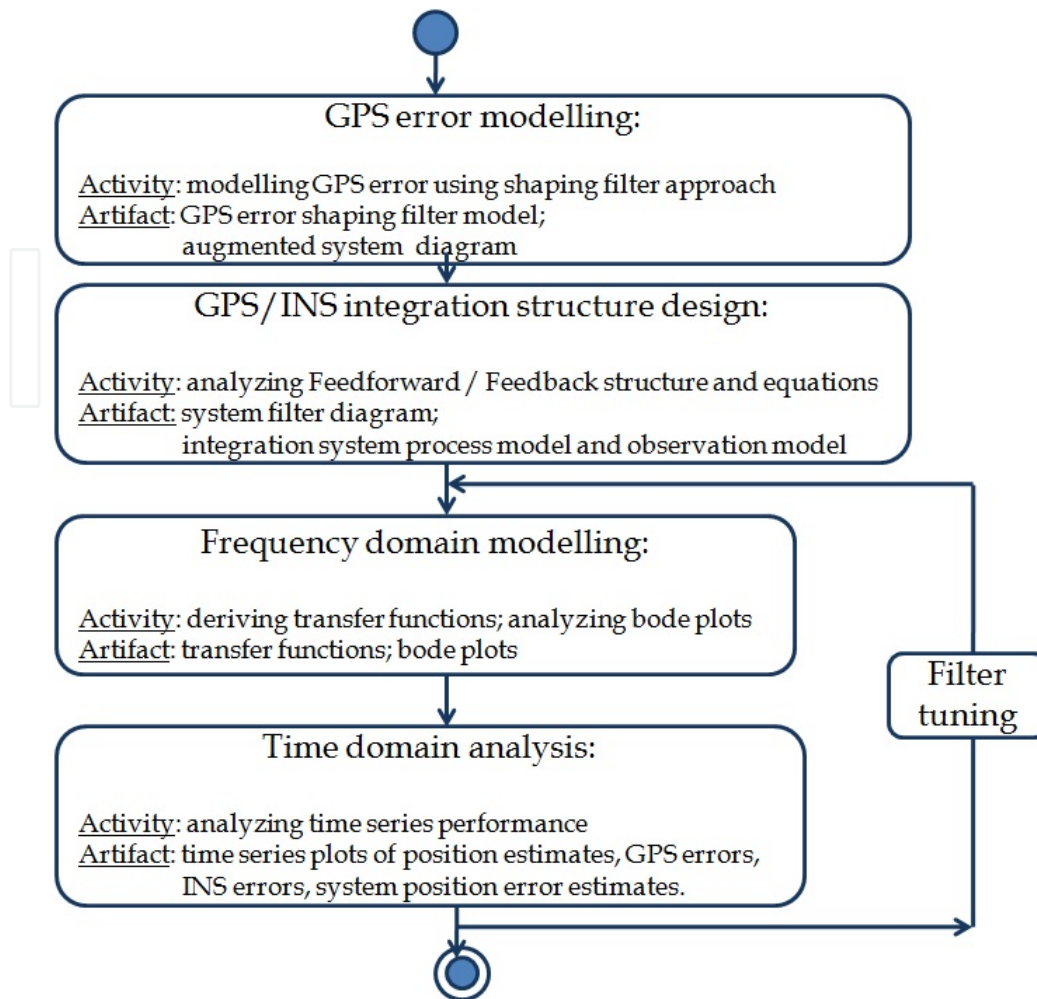


Figure 14. Activities and associated artifacts in the positioning error de-correlation process

As demonstrated in the previous sections of this chapter, this process includes the following major activities.

Activity 1: GPS error modelling using shaping filter approach. The associated artifacts of this activity include a GPS error shaping filter model and an augmented system diagram using this shaping filter.

Activity 2: GPS/INS integration design by analyzing the feedforward or feedback structures and their equations. The artifacts of this design activity are a system filter structure diagram, a set of filter equations of the process model and observation model.

Activity 3: Frequency domain modelling by deriving transfer functions and analyzing bode plots. The artifacts in frequency domain are transfer functions of the filter state estimates over filter measurement inputs, and bode plots using these transfer functions.

Activity 4: Time domain analysis by verifying the time series performance. The artifacts of this activity include a set of time series plots. These plots illustrate the GPS errors, INS errors, system errors, and system positioning estimates over time.

During this process, the artifacts in Activity 3 and Activity 4 will be iteratively analyzed using filter tuning with the trial of sensor noise levels. The system error de-correlation process stops once the threshold of the sensor noise level is found, and the final system accuracy level meets the system requirements.

6. Conclusions

This chapter presents a positioning system error de-correlation process approach. The aim of this approach is to solve the accuracy and availability issues of GPS based positioning system. In this chapter, this approach is standardized into an engineering process with a number of activities and associated artifacts. This approach starts from system component level by modelling GPS errors. GPS error is modelled using shaping filter approach. The artifact of GPS error modelling is an augmented system with the GPS error shaping filter. Once the component model is understood, the GPS/INS integration structures are analyzed at system high level. Feedforward filter and feedback filter structures are analyzed, designed and implemented for their benefits. Under each feedforward or feedback filter structure, the integrated system performance is analyzed both in frequency domain and time domain. The analysis activities are designed in an iterative filter tuning process. INS plays a role with its noise level in filter tuning process in both feedforward and feedback filter structures. Using the GPS/INS error de-correlation approach in this chapter, the experiments demonstrate that the final system accuracy level is improved.

This approach is designed for GPS/INS integration system. Further research could be extending this engineering process to other positioning sensor integration systems.

Author details

Xiaoying Kong
University of Technology, Sydney, Australia

Li Liu
The University of Sydney, Australia

Heung-Gyoon Ryu
Chungbuk National University, South Korea

7. References

- Alban, S.; Akos, D.; Rock, S. & Gebre-Egziobher, D. (2003). Performance Analysis and Architectures for INS-Aided GPS tracking loops, Institute of Navigation - NTM, Anaheim, CA, 22-24 January, 2003, pp. 611-622
- Committee on Oversight and Government Reform (2009). Hearing on GPS: can we avoid a gap in service? Last accessed: 13/4/2012. Available from: U.S. House of Representatives web site, <http://oversight.house.gov/hearing/gps-can-we-avoid-a-gap-in-service/>

- Federal Aviation Administration (2012). WAAS Test Team Website, Last accessed: 13/4/2012. Available from: <http://www.nstb.tc.faa.gov/>
- GAO (2009). Global positioning system, significant challenges in sustaining and upgrading widely used capabilities, United States Government Accountability Office report, GAO-09670T
- Gaylor D.; Lightsey G. & Key K. (2005). Effects of multipath and signal blockage on GPS navigation in the vicinity of the International Space Station (ISS), *Journal of The Institute of Navigation*, Summer 2005, Vol. 52, No. 2, pp. 61-70
- Geiger, W.; Bartholomeyczik, J.; Breng, U.; Gutmann, W.; Hafen, M.; Handrich, E.; Huber, M.; Jackle, A.; Kempfer, U.; Kopmann, H.; Kunz, J.; Leinfelder, P.; Ohmberger, R.; Probst, U.; Ruf, M.; Spahlinger, G.; Rasch, A.; Straub-Kalthoff, J.; Stroda, M.; Stumpf, K.; Weber, C.; Zimmermann, M.; Zimmermann, S. (2008). MEMS IMU for AHRS applications, 2008 IEEE/ION on Position, Location and Navigation Symposium, 5-8 May 2008; pp. 225 - 231; Monterey, CA
- Groves, P. (2005). GPS signal-to-noise measurement in weak signal and high-interference environments, *Journal of The Institute of Navigation*, Summer 2005, Vol. 52, No. 2, pp. 83-94
- Kong, X.; Nebot E. & Durrant-Whyte H. (1999). Development of a non-linear psi-angle model for large misalignment errors and its application in INS alignment and calibration, *Proceedings of IEEE International Conference on Robotics and Automation*, Detroit, MI, USA, May, 1999, pp. 1430-1435
- Kong, X.; Liu, L. & Tran., T. (2010). Modeling satellite Positioning errors in different configurations from end user's viewpoint, *Proceedings of the 16th Asia-Pacific Conference on Communications (APCC 2010)*, Oct. 31 -Nov. 3 2010, Auckland
- Lashley, M.; Bevly, D. & Hung, J. (2010). Analysis of Deeply Integrated and Tightly Coupled Architectures, *Proceedings of IEEE/ION PLANS 2010*, pp.382-396, May 4-6, 2010
- Maybeck, P. (1979). *Stochastic models, estimation and control*, New York, Academic Press, 1979
- Nebot, E.; Durrant-Whyte, H. & Scheduling S. (1996). Kalman filtering design techniques for aided GPS land navigation applications, *Data Fusion Symposium, 1996. ADFS'96*, First Australian.
- Nebot E. & Durrant-Whyte H. (1999). Initial calibration and alignment of low cost inertial navigation units for land vehicle applications, *Journal of Robotics Systems*, Vol. 16, No. 2, Feb. 1999, pp. 81-92
- Owen, J. & Wells, M. (2001). An advanced digital antenna control unit for GPS". IN: *Look at the changing landscape of navigation technology; Proceedings of the Institute of Navigation 2001 National Technical Meeting*, Long Beach, CA, Jan. 22-24, 2001, Alexandria, VA, Institute of Navigation, 2001, pp. 402-407
- Rose, J.; Allain, D. & Mitchell, C. (2009). Reduction in the ionospheric error for a single-frequency GPS timing solution using tomography, *Annals of Geophysics*, Vol 52, No 5, 2009

- Sahawneh, L. & Jarrah, M.A. (2008). Development and calibration of low cost MEMS IMU for UAV applications, 5th International Symposium on Mechatronics and Its Applications, 2008. ISMA 2008; 27-29 May, 2008
- Scheding, S. (1997). PhD thesis, High Integrity Navigation, The University of Sydney, 1997
- Scheding, S.; Nebot, E.; Stevens, M.; Durrant-Whyte, H.; Roberts, J. & Corke, P. (1997). Experiments in autonomous underground guidance, IEEE International conference on Robotic and Automation, Albuquerque, NM, USA, Apr. 1997, pp. 1898-1903
- Sukkarieh, S. (2000). Low Cost, High Integrity, Aided Inertial Navigation Systems for Autonomous Land Vehicles. PhD thesis, The University of Sydney, 2000
- Wikipedia (2012). Differential GPS, Last accessed: 12/4/2012, Available from: http://en.wikipedia.org/wiki/Differential_GPS
- Wikipedia (2012). Global Positioning System, Last accessed: 13/4/2012. Available from: http://en.wikipedia.org/wiki/Global_Positioning_System
- Wu, J. & Hsieh, C. (2010). "Statistical modeling for the mitigation of GPS multipath delays from day-to-day range measurements", JOURNAL OF GEODESY Volume 84, Number 4, pp. 223-232, DOI: 10.1007/s00190-009-0358-6